

Morphological and molecular evidence of cryptic speciation in sympatric colour morphotypes of *Mycale (Carmia) cecilia* (Porifera: Poecilosclerida) from the Mexican Pacific

Ana Castillo-Páez, Raúl Llera-Herrera, José Antonio Cruz-Barraza

Institute of Marine Sciences and Limnology, Mazatlán Academic Unit, National Autonomous University of Mexico, avenida Joel Montes Camarena s/n, Mazatlán, Sinaloa, CP 82000, Mexico.

(AC-P) E-mail: anacastillopaez@hotmail.com. ORCID iD: <https://orcid.org/0000-0003-4428-2217>

(RL-H) E-mail: raul.llera@ola.icmyl.unam.mx ORCID iD: <https://orcid.org/0000-0001-9873-9732>

(JAC-B) (Corresponding author) E-mail: joseantonio@ola.icmyl.unam.mx. ORCID iD: <https://orcid.org/0000-0001-5472-3288>

Summary: Identifying cryptic species is pivotal for understanding marine biodiversity and optimizing strategies for its conservation. A robust understanding of poriferan diversity is a complex endeavour. It has also been extremely hampered by the high phenotypic plasticity and the limited number of diagnostic characters. *Mycale (Carmia) cecilia* has different body colours, even among individuals living together. We tested whether the colour variation could be due to polymorphism, phenotypic plasticity or cryptic speciation. Phylogenetic reconstructions of nuclear and mitochondrial loci were congruent. Individuals of different body colour did not cluster together and had high levels of genetic divergence. Furthermore, the green morphotype clustered in almost all reconstructions with *Mycale (C.) phyllophila*, as both showed higher gene similarity at the transcriptomic level (public transcriptome). Morphologically, the green individuals consistently showed discrepancies from the red ones. These results suggest that all individuals with the same body colour, either red or green, correspond to the same species, while individuals with different body colours probably belong to different species. These results reveal high levels of morphologic and genetic diversity, which could have important implications for what is known as *M. (C.) cecilia* and the Mycalidae systematics.

Keywords: Porifera; anisochelae categories; cryptic species; COI, 28S rRNA; *ITS1*; colour morphotype; transcriptomics.

Evidencia morfológica y molecular de especiación críptica en morfotipos de colores simpátricos de *Mycale (Carmia) cecilia* (Porifera: Poecilosclerida) del Pacífico mexicano

Resumen: Identificar especies crípticas es fundamental para comprender la biodiversidad marina y optimizar estrategias para su conservación. Una comprensión sólida de la diversidad de los poríferos es una tarea compleja; puesto que ha sido extremadamente obstaculizada debido a la alta plasticidad fenotípica y al número limitado de caracteres diagnósticos. *Mycale (Carmia) cecilia* tiene diferentes colores corporales incluso en individuos que viven uno al lado del otro. Probamos si la variación de color podría deberse a polimorfismos, plasticidad fenotípica o especiación críptica. Las reconstrucciones filogenéticas de loci nucleares y mitocondriales fueron congruentes. Los individuos de diferente color corporal no se agrupaban y tenían altos niveles de divergencia genética. El morfotipo verde se agrupó en casi todas las reconstrucciones con *Mycale (C.) phyllophila*, mostrando también una elevada similitud genética a nivel transcriptómico (transcriptoma público). Morfológicamente, los individuos verdes mostraron consistentemente discrepancias con los individuos rojos. Estos resultados sugieren que todos los individuos con el mismo color corporal ya sea rojo o verde corresponden a la misma especie, mientras que los individuos con diferentes colores corporales probablemente pertenecen a especies diferentes. Estos resultados revelan altos niveles de diversidad morfológica y genética, lo que podría tener implicaciones importantes para lo que se conoce como *M. (C.) cecilia* y la sistemática Mycalidae.

Palabras clave: Porifera; categorías de anisochelae; especies crípticas; COI, ARNr 28S, *ITS1*, morfotipo de color; transcriptómica.

Citation/Como citar este artículo: Castillo-Páez A., Llera-Herrera R., Cruz-Barraza J.A. 2024. Morphological and molecular evidence of cryptic speciation in sympatric colour morphotypes of *Mycale (Carmia) cecilia* (Porifera: Poecilosclerida) from the Mexican Pacific. Sci. Mar. 88(1): e082. <https://doi.org/10.3989/scimar.05339.082>

Editor: M. Pascual.

Received: September 20, 2022. **Accepted:** December 18, 2023. **Published:** March 15, 2024.

Copyright: © 2024 CSIC. This is an open-access article distributed under the terms of the Creative Commons Attribution 4.0 International (CC BY 4.0) License.

INTRODUCTION

Establishing the species boundaries between a set of morphologically similar individuals and inferring the number of extant species is essential for biodiversity conservation (De Queiroz 2007, Petit and Excoffier 2009). However, when species are not well delimited, biodiversity is underestimated, so ecological interactions could remain hidden, and conservation actions could be inappropriate (Pfenninger and Schwenk 2007). Cryptic species are two or more distinct species that are difficult or impossible to distinguish owing to morphological similarity and are therefore erroneously classified as a single nominal species (Knowlton 1993, Bickford et al. 2006). In contrast, some species have a high degree of phenotypic variation, which is the ability of a genotype to display different phenotypes depending on the biotic or abiotic environmental conditions (Fusco and Minelli 2010). Commonly, these phenotypes are incorrectly identified as different species.

When cryptic species are ignored, i) the number of species in a community could be underestimated, altering the species richness index that is considered an indicator of good ecological status; ii) the overestimation of a given species because the cryptic species that compose it are ignored affects the estimation of biological parameters such as abundance, population size, population connectivity, range size and geographical range; and iii) speciation rates could be incorrectly detected, leading to false inferences about important evolutionary processes (Chenauil et al. 2019).

Porifera is a complicated group because of the morphological simplicity and phenotypic plasticity exhibited by many of its species. Sponge systematics is based mainly on the composition of the skeleton and structure. Traditionally, spicules (morphology and size) and spongin fibers have been useful as taxonomic characters, especially when they have many different types and a complex skeletal organization or structure (Cárdenas et al. 2012). With the development of molecular tools, the systematic description of new species has incorporated DNA barcodes and other molecular markers from the mitochondrial or nuclear genomes to strengthen taxonomic hypotheses on species delimitation; these markers are sequences specifically obtained from individuals used to describe the species (Blanquer and Uriz 2008, Cárdenas et al. 2012).

Genomic and genetic approaches are powerful tools for resolving the relationship of individuals that have similar morphology. In recent decades, they have been used to resolve cryptic speciation and phenotypic plasticity in marine sponges. For instance, phylogenetic reconstruction of *Scopalina lophyropoda* individuals revealed four differentiated clades; the large genetic differences between groups with no shared haplotypes suggest that each clade is a different species. One of them is sympatric with *S. lophyropoda* (Blanquer and Uriz 2007).

Moreover, molecular studies reveal the morphological complexity of several sponge species; for example, *Cliona viridis* is a species complex, the species are

grouped on the basis of morphological similarities, and all of them show considerable intragenomic variation and had a polyphyletic placement in the genealogies and very low divergence; some species had overlapped interspecific variation with intraspecific variation (Escobar et al. 2012). The phenotypic plasticity has also been evaluated with genetic markers; another example is *Callyspongia vaginalis*, with three morphotypes (colours and shapes) without genetic differentiation between them (López-Legentil et al. 2010). Until today, no marine sponge studies have used an “omic” data set to discriminate species. In particular, transcriptome-derived markers are useful in species with slow evolution rates, such as Porifera (Huang et al. 2008, Kenny and Itskovich 2020).

The genus *Mycale* is subdivided into 11 subgenera characterized by the combination of the morphology of the spicules and details of their skeletal arrangement (Van Soest and Hajdu 2002). *Mycale (Carmia) cecilia* (de Laubenfels 1936) belongs to the subgenus *Carmia*, which includes species with a plumose or plumoreticulated choanosomal skeleton; the ectosomal skeleton is absent or evident with only a few scattered mycalostyles in one category or palmate anisochelae in one or more size categories, the larger size can form rosettes; some species may also have sigmas, toxas, raphides and micracanthoxeas (Hajdu and Riitzler 1998). *Mycale* species have pharmacological potential because of the production of mycalamides metabolites. Particularly, *M. (C.) cecilia* produces pyrrole-2-carbaldehyde derivatives that have growth inhibitor activity in certain human prostate carcinomas (Ortega et al. 2004).

Mycale (C.) cecilia was described by de Laubenfels (1936) on the Pacific coast of Panama. According to the original description, the species has a green coloration in life, with red specks on the surface that are probably embryos. It has a mycalostyle size ranging from 7 by 300 μm to 10 by 300 μm ; very narrow palmate anisochelae in two sizes, from 12 to 15 μm and 22 to 25 μm , and sigmas of around 30 μm length. The species is abundant in rocks of the intertidal zone (de Laubenfels 1936). The same author recorded a few specimens of *M. (C.) cecilia* in mangrove roots in Hawaii (de Laubenfels 1950). The specimen spicules showed length variation in comparison with the Panama specimens; the mycalostyles had long heads (4-6 by 240-250 μm); sigmas ranging from 30 to 42 μm length; and a single size category of palmate anisochelae that varied between individuals. The Hawaiian specimens were of different colours, including pink, lavender, yellow, orange and red, but never green. De Laubenfels (1950) suggested that the coloration may change with age, reproduction or algal symbionts, as did the green ones in Panama. The most southern record of *M. (C.) cecilia* is a preserved Galapagos Islands specimen. It had mycalostyles of 166-230-260 by 2-4 μm , sigmas from 24 to 35 μm length (mean 30 μm), and palmate anisochelae of 10-20 μm length (mean 14 μm), which according to the authors, possibly had two size categories but without a clear bimodal display (Desqueyroux-Faúndez and van Soest 1997).

Green and Gomez (1985) described organisms from Mazatlán, nominating them as *M. microsigmatosa*; those individuals had bright red and orange body colours. However, Hajdu and Riitzler (1998) synonymize those organisms as *M. (C.) cecilia*. This species is widely distributed in the Mexican Pacific; coloration varies between individuals: red to reddish-orange, green with yellow or blue, but always with small orange, yellow or red mottled patchwork. Mycalostyles had 130-290 by 2.1-8.8 μm length and width and palmate anisochelae in one category from 12.5 to 27.5 μm length, and sigmas ranged from 15 to 50 μm (Carballo and Cruz-Barraza 2010). This phenotypic variation (at least for the body colour) of *M. (C.) cecilia* in the Eastern Pacific Ocean has also been observed in other affine species, such as *M. microsigmatosa* (reviewed by Hajdu and Riitzler 1998) in the Caribbean and *M. (C.) phyllophila* (Van Soest and Hajdu 2002) in the Indo-Pacific.

Our contribution aimed to evaluate whether organisms of *M. (C.) cecilia* with different body colours but living side by side depict different morphotypes of a single species and are a display of phenotypic plasticity. This hypothesis was tested using two approaches:

micromorphometric analysis of spicules (traditional taxonomy) and multilocus analysis of genetic divergence (DNA and RNA).

MATERIALS AND METHODS

Collection of material

Eight individuals of *M. (C.) cecilia* were collected in the morning on the same day (26 July 2019) from the Urias Estuary in Mazatlán, Sinaloa, Mexico (23°11'07.3"N, 106°25'18.4"W). The sponges were found side by side, between one and two meters deep in an artificial jetty. We chose eight individuals: four with red body colour and red to reddish-orange specks and four with green body colour and green to greenish-yellow specks (Fig. 1). Hereafter, these are referred to as red (MCR) and green (MCG) morphotypes, respectively. The samples were transported to the laboratory in an aerated seawater aquarium. For morphological analysis and DNA extraction, a small fragment of each individual was fixed in 70% and 96% ethanol, respectively. For transcriptome analysis, a small portion of

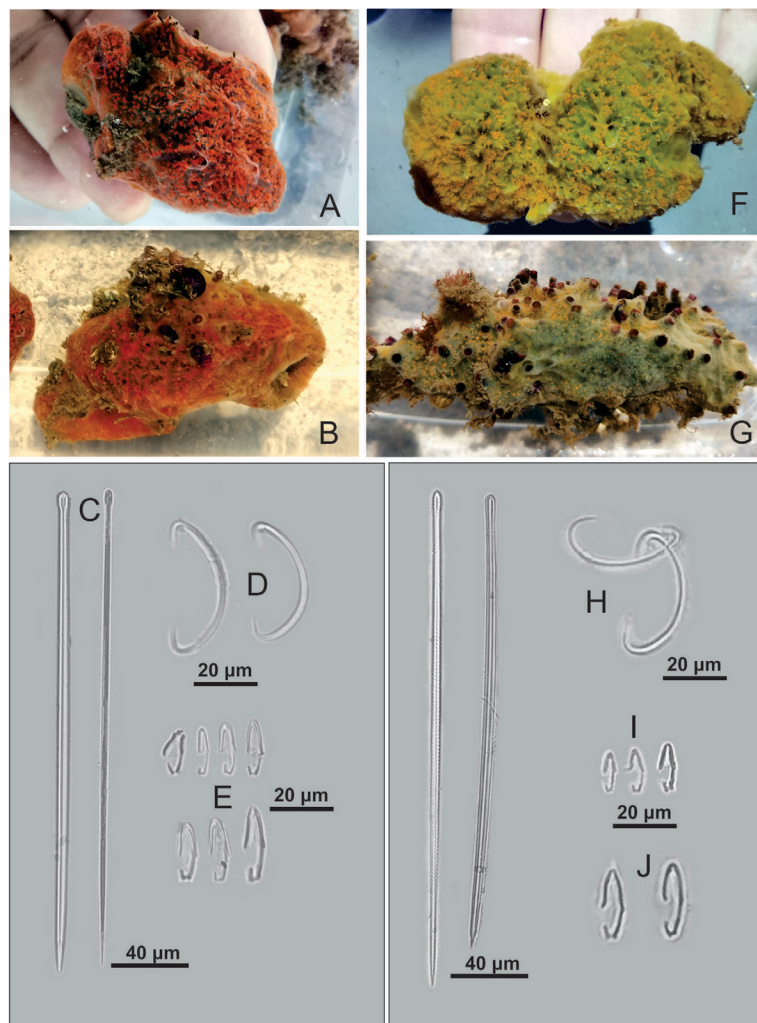


Fig. 1. – External morphology of *Mycale (C.) cecilia* from Mazatlán, Mexican Pacific. Red to reddish-orange morphotype (A-E) and green to greenish-yellow morphotype (F-J).

50–100 µg of each fresh individual was dissected using a stereoscope to avoid macrosymbionts; the tissue was immediately homogenized in 1 mL of TRIzol™ Reagent (Thermo Scientific; Waltham, MA) and stored at -20°C until RNA isolation. All specimens were deposited in the Mexican Pacific Sponge Collection held by the Institute of Marine Sciences and Limnology, National Autonomous University of Mexico (red morphotype, LEB-ICML-UNAM-3181 MCR1 to MCR4 and green morphotype, LEB-ICML-UNAM-3182 MCG5 to MCG8).

Transcriptome analysis

Three individuals of each morphotype were used for RNA isolation for standard RNA-seq, library preparation and sequencing. Raw reads of three individuals of each morphotype were pooled for transcriptome assembly and biological contamination detection based on Porifera best-hit. These procedures were performed and described in Castillo-Páez et al. (2021). The raw reads of the transcriptomes for the pre-competent larvae, post-larvae and adults of *Mycale (Carmia) phyllophila* (NCBI SRA BioProject: PRJNA269144; accessed on 10 August 2020) were assembled and used as comparative material. The Porifera open reading frames (ORFs) of each transcriptome of *M. (C.) cecilia* and the *M. (C.) phyllophila* transcripts were used to identify orthologous by bidirectional reciprocal BLAST hit to obtain pairs of sequences with the best hit (E-value of $1e^{-5}$). Histograms were used to present the numbers of ORFs and the percentage of amino acid identity for each transcriptome comparison (i. *M. (C.) cecilia* green vs. *M. (C.) cecilia* red; ii. *M. (C.) cecilia* green vs. *M. (C.) phyllophila*; and iii. *M. (C.) cecilia* red vs. *M. (C.) phyllophila*).

To confirm speciation trends between the two morphotypes based on phylogenetic inference of single-copy orthologous genes, we retrieved RNA-seq from the NCBI SRA BioProject (accessed on 4 August 2023) for *Mycale grandis* (PRJNA317402), *Mycale laevis* (PRJNA612016), *Mycale acerata* (PRJNA612010) and *Mycale tridens* (PRJNA612015) and *Clathria prolifera* (PRJNA901949) as an outgroup. The raw reads were transformed to paired-end .fastq files and individually assembled with Trinity software v2.15.1 (Haas et al. 2013), using the -trinode option without considering the strand-specific orientation of reads. The obtained transcriptome assemblies were assessed for basic metrics with the Trinitystats.pl script. The conceptual translations of proteins were processed with Transdecoder v. 5.7.0 included in Trinity software, retaining the HMMER and blastp hits against pFAM and UniProt-SwissProt, respectively. Only the proteins annotated as “complete” by the Transdecoder tool were retrieved for further analysis. We used the OrthoFinder tool (Emms and Kelly 2019) to assess the potential orthogroups among all the included species (FastME option) or a selection of those more closely related to *M. (C.) cecilia* morphotypes. A gene tree was obtained using the STAG approach (Emms and Kelly

2017, Emms and Kelly 2018), in which the most likely phylogenomic relationship’s tree is obtained by collapsing individual trees obtained by all the single-copy orthologous genes. A detailed description of the retrieved RNA-seq NCBI SRA accessions and assembly metrics and the scripts and commands used to create the protein collection for each species are presented in Supplementary Material Table S1 and Table S2.

DNA extraction and *ITS1* amplification and sequencing

Total DNA was extracted for preserved tissues (70% ethanol) using the Quick-DNA™ Fecal/Soil Microbe Kits (Zymo Research, Orange, CA, USA) according to the manufacturer’s protocol. The Internal Transcribed Spacer 1 (*ITS1*) locus was amplified with primers designed by Adlard and Lester (1995) *RA2* 5'-GTCCCTGCCCTTGTACACA-3' and *ITS2.2* 5'-CCTGGTTAGTTTCTTTTCTCCGC-3'. PCR reactions were conducted in a final volume of 15 µL containing ~20 ng of template DNA, 1x NH4 buffer (Bioline), 2 mM MgCl₂, 0.2 mM dNTP, 0.4 µM of each primer, and 0.5 U of MyTaq DNA polymerase (Bioline). Amplification conditions were: 95°C for 5 min; then 35 cycles of 94°C for 30 s, 49°C for 30 s and 68°C for 1 min; and a final elongation step of 72°C for 10 min. Because of unspecific bands, PCR products were separated by electrophoresis in 1.5% agarose gels. DNA bands were recovered with the Wizard® SV Gel and PCR Clean-Up System (Promega, Madison, WI, USA) and were processed by capillary sequencing through a third-party service at Macrogen Inc. (Korea).

Phylogenetic relationships and species delimitation based on traditional loci

Genetic loci traditionally used in phylogenetic studies were recovered from each transcript set [nuclear *18S* and *28S* rRNA and mitochondrial *16S* rRNA and cytochrome c oxidase subunit 1 (*COX1*) genes] or Sanger sequences for *ITS1* (MCR and MCG). BLASTx searches were performed using *Mycale* spp. sequences downloaded from GenBank as a reference for each genetic marker. Genetic distances were calculated with the uncorrected p-distance index for each marker, assuming uniform rates among sites and conducting pairwise deletion of gaps and missing data. The best-fitting DNA substitution model was inferred from the complete alignments using an initial neighbour-joining tree and the maximum likelihood statistical method using all sites, and a strong branch swap was used for gaps and missing data (5 threads). Phylogenetic reconstructions were made from each complete alignment with the maximum likelihood method with 300 bootstrap replicates using the best-fitting substitution model defined previously, and the tree inference nearest-neighbour-interchange with a very strong branch swap filter. These analyses were done in MEGA X (Kumar et al. 2018). Assemble Species by Automatic Partitioning (ASAP) software on the web server was run for species

delimitation, applying the Kimura (K80 ts/tv 2.0) substitution model to compute the distances (Puillandre et al. 2021).

Morphology and spicule size

Spicule preparations were made following the techniques described by Carballo and Cruz-Barraza (2008). The different types of spicules were visualized under an Olympus® CX21 light microscope with an ocular micrometer rule. Twenty-five mycalostyles, 25 sigmas and 50 palmate anisochelae were randomly measured for each individual. Length, shaft width and head width were measured for each mycalostyle. Total and head lengths were taken for palmate anisochelae. For sigmas, only the length was recorded. A histogram was used to visualize the frequency and density of the spicule sizes. Statistical analyses were conducted to test significant differences in the spicular mean between individuals. After evaluating the homoscedasticity with the Bartlett test or Fligner-Killeen test, transformations (natural logarithm or square root) were implemented for normalization. We used analysis of variance with a significance level of 0.05. An a posteriori Tukey HSD test was conducted to identify the most different individuals. The multidimensional distribution of the samples based on morphometric data was explored using a principal component analysis (PCA). All analyses were performed in RStudio (version 1.2.5001, RStudio, Inc.).

RESULTS

Phylogenetic relationships and species delimitation inferred from traditional loci

Sequences from *ITS1* were successfully obtained for all specimens examined. *ITS1* sequences from the red individuals were 332 nt long, and those from the green individuals were 333 or 334 nt long. The number of differences (0 to 1) and genetic distances (0% to 0.3%) within each colour (red or green) morphotype group was extremely low when they occurred. However, when comparisons were made between individuals of different morphotypes of *M. (C.) cecilia*, the substitutions and differences were more evident (MCR vs. MCG in Table 1). Notably, the differences between *M. (C.) cecilia* morphotypes (MCR vs. MCG) were greater than those between MCG and *M. (C.) phyllophila* (Table 1). This locus was highly variable compared with the other analysed genes. The best-fitting substitution model was T92 + I. Individuals of *M. (C.) cecilia* with the same colour were grouped in a strongly supported monophyletic clade (bootstrap value 100%, Fig. 2). *M. (C.) phyllophila* clustered into the MCG clade, suggesting that this is a sister species to MCG. Four best partitions were found by ASAP for the *ITS* region sequences. The first partition was the best supported (p-value <0.05) and indicated that there were six subsets. In one of them there were only the samples of the green morphotype and in another only the samples of

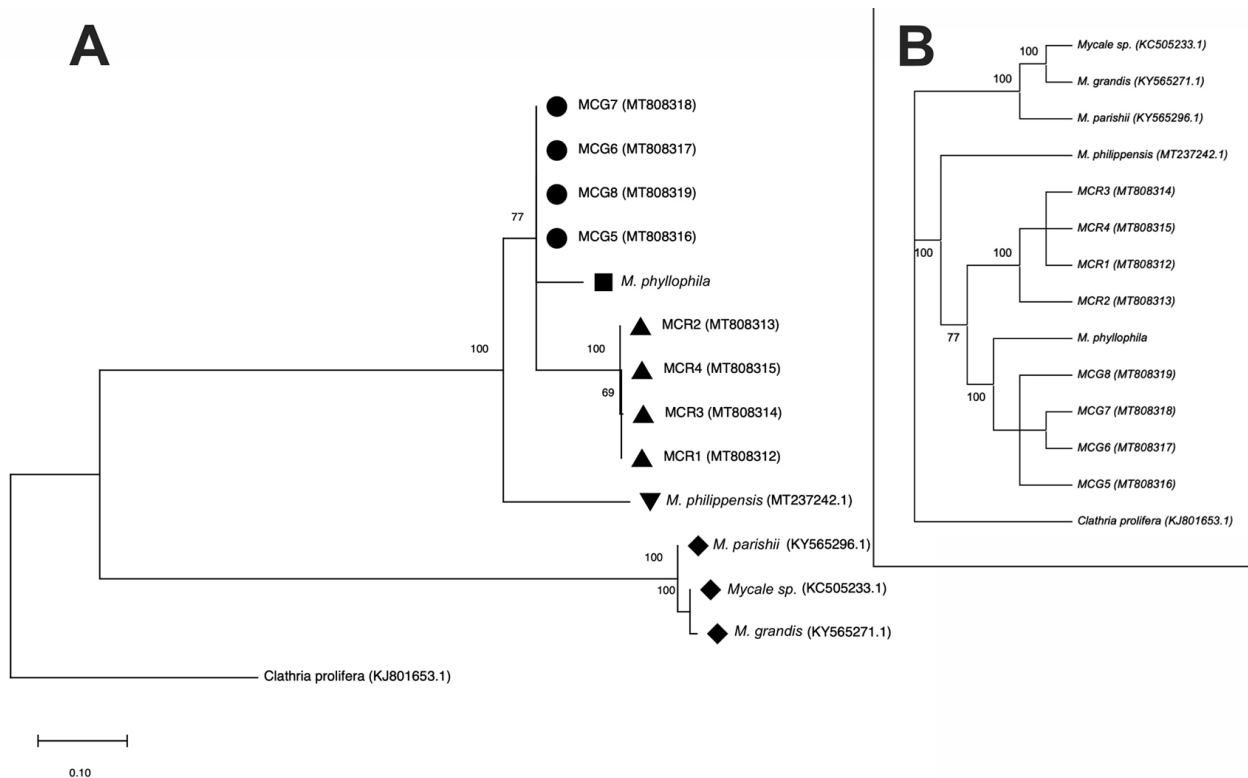


Fig. 2. – Maximum likelihood phylogenetic reconstruction for nuclear locus *ITS1* ML (A) and bootstrap consensus (B) for morphotypes for *Mycale (C.) cecilia* (MCR, red individuals; MCG, green individuals) and other species of *Mycale*. GenBank accession numbers in parentheses. Values in the nodes indicate Bootstrap support (>75%, 300 replicates). Symbols indicate species/clusters identified based on ASAP.

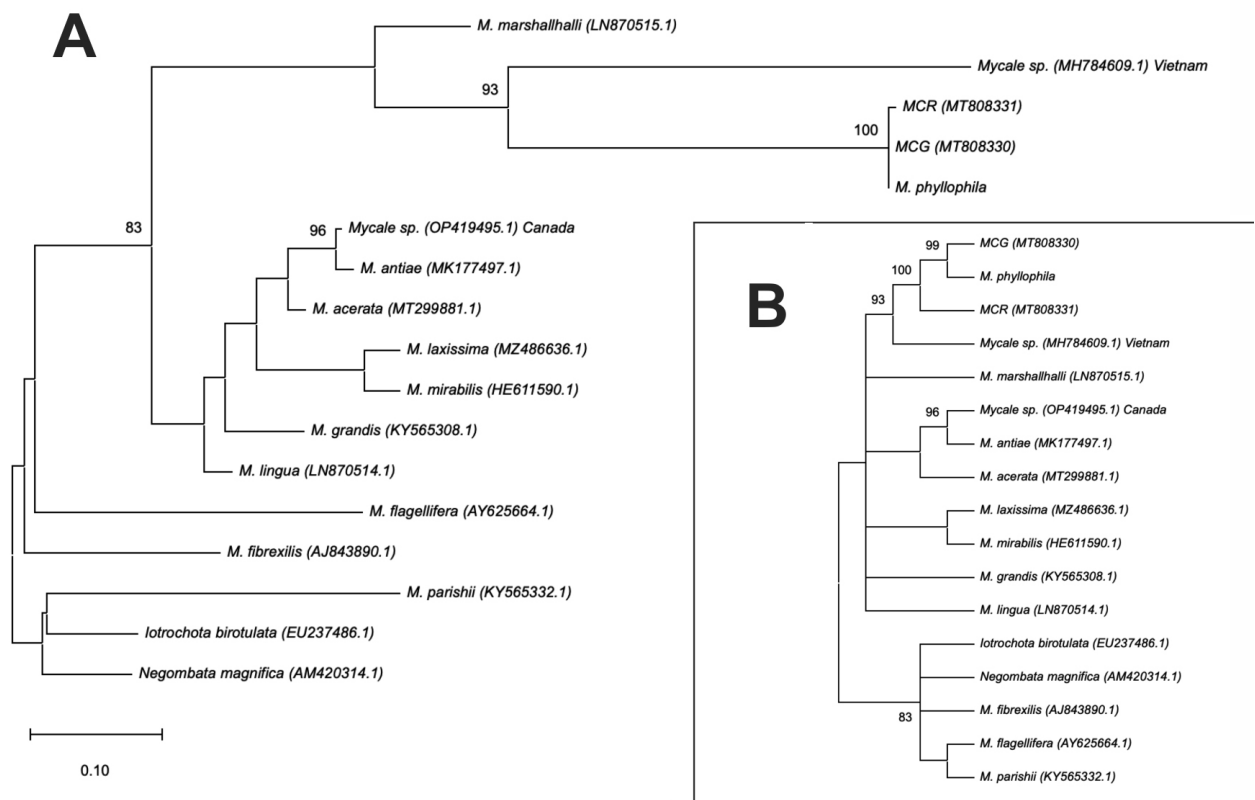


Fig. 4. – Maximum likelihood phylogenetic reconstruction for COI gen (A) and bootstrap consensus (B) for morphotypes for *Mycale (C.) cecilia* (MCR, red individuals; MCG, green individuals) and other species of *Mycale*. GenBank accession numbers are in parentheses. Values in the nodes indicate Bootstrap support (>75%, 300 replicates).

Table 1. – Genetic distances and number of substitutions of *M. (C.) cecilia* morphotypes and other *Mycale* species. Gen. dis, genetic distance; N. sub, number of substitutions; MP, *M. (C.) phyllophila*; OM, a species of *Mycale* other than *M. (C.) phyllophila*; (*), *ITS* is the only gene with more than one sequence (eight in total).

Comparison	Locus	Gen. dis	N. sub.	Locus	Gen. dis	N. sub.
MCR vs. MCG		7.93 to 8.79	26 to 28		0.81	14
MCG vs. MP		4.82 to 4.83	16		0	0
MCR vs. MP	<i>ITS*</i>	11.28 to 11.59	37 or 38	<i>18S</i>	0.81	14
MCG vs. OM		14.19 to 45.06	44 to 146		0 to 5.56	0 to 90
MCR vs. OM		20.97 to 43.61	65 to 140		0 to 5.21	0 to 96
MCR vs. MCG		1.33	12		0	0
MCG vs. MP		0	0		0.23	1
MCR vs. MP	<i>28S</i> D1-D2	1.33	12	<i>28S</i> D3-D5	0.23	1
MCG vs. OM		3.54 to 23.19	32 to 186		0.24 to 2.86	1 to 12
MCR vs. OM		2.55 to 23.22	23 to 186		0.24 to 2.86	1 to 12
MCR vs. MCG		0.5	7		0.17	1
MCG vs. MP		0	0		0	0
MCR vs. MP	<i>COXI</i>	0.5	7	<i>16S</i>	0.17	1
MCG vs. OM		19.93 to 27.09	110 to 175		0 to 15.14	0 to 90
MCR vs. OM		19.93 to 27.09	111 to 175		0 to 15.14	0 to 90

the red morphotype. *M. phyllophila* did not group with the green morphotype.

The partial consensus sequences for *M. (C.) cecilia* from the 28S rRNA D1-D2 domain had a length of 905 nt. The best-fitting model of substitution was TN93+G. The sequences were identical between MCG and *M. (C.) phyllophila* (Table 1). In addition, a low value was observed in pairwise comparisons between the morphotypes (MCR and MCG) of *M. (C.) cecilia*, and this value was the lowest when compared with another *Mycala* spp. (except *M. (C.) phyllophila*). The phylogenetic construction was well resolved. Both the morphotypes and *M. phyllophila* were clustered, although MCG and *M. phyllophila* may be siblings because they clustered in a highly supported branch (100% bootstrap, Fig. 3). Nine partitions were detected by ASAP analyses, but they were not informative (p-value > 0.1).

The other domain (D3-D5) was not informative, as no nucleotide differences were found between morphotypes or in other species, such as *M. mirabilis* vs. *M. setosa*, *M. fistulifera* vs. *M. microsigmatosa* and *M. (C.) cecilia* from Hawaii (KC961688.1) vs. *M. adhaerens*. Phylogenetic reconstruction was performed with 420 nt. The best-fitting model was K2+G+I. None of the clades was well supported and all bootstrap values were less than 75% (even 0). However, the two morphotypes (MCR and MCG) clustered in a moderately supported clade (65% bootstrap; Fig. S1). Partitions

detected for species delimitation were not useful. The two morphotypes were clustered even with other *Mycala* species.

Partial consensus sequences of the 18S rRNA gene (1728 nt) for each morphotype were retrieved from the assembled transcriptome. The uncorrected p-distances ranged between 0% and 5.6% (Table 1). The lowest value was found between MCG and *M. (C.) phyllophila*, where sequences were identical. The genetic distance between MCR and MCG was slightly higher than that between other species, i.e. MCG vs. *M. microsigmatosa* (0.17) or *M. sanguinea* (0.23). We found 14 substitutions between *M. (C.) cecilia* morphotypes and none between *M. (C.) phyllophila* and MCG. The best-fitting model of substitution was K2+G+I. The phylogenetic reconstruction had low support values but was useful to show that our morphotypes were not monophyletic. MCG vs. *M. (C.) phyllophila* clustered with a high bootstrap value (Fig. S2). The species delimitation analysis was not congruent; the two morphotypes were grouped even with other *Mycala* species.

We analysed two mitochondrial genes. *COX1* was more informative than the 16S rRNA gene. For *COX1*, there were seven substitutions at 1261 nt between MCR and MCG. The sequences were identical between MCG and *M. (C.) phyllophila* (Table 1). The phylogenetic tree was made with HKY+G as the best-fitting substitution model. Both *M. (C.) cecilia* and *M. (C.) phyllophila*

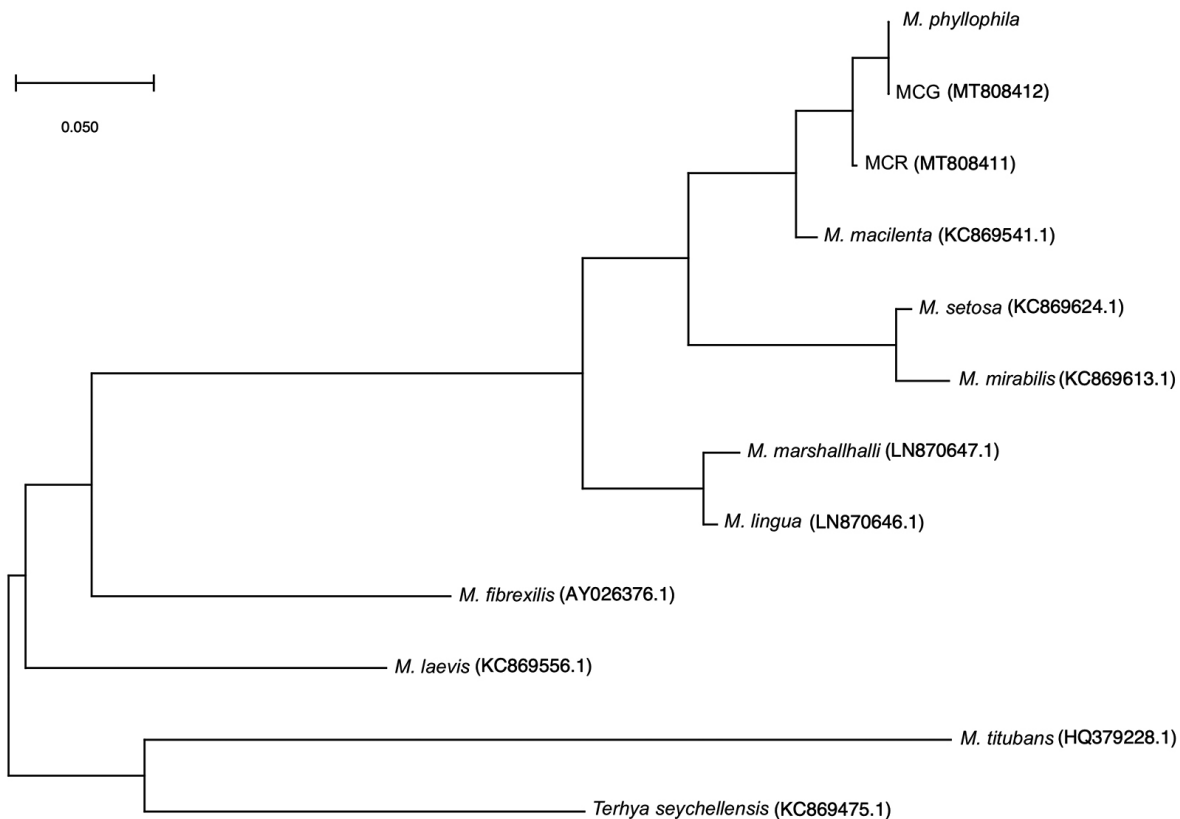


Fig. 3. – Maximum likelihood phylogenetic reconstruction of the partial D1-D2 domain of the 28S gene among morphotypes of *Mycala cecilia* (MCR, red individuals; MCG, green individuals) and other species of *Mycala*. Values in the nodes indicate bootstrap support (300 replicates). GenBank accession numbers in parentheses.

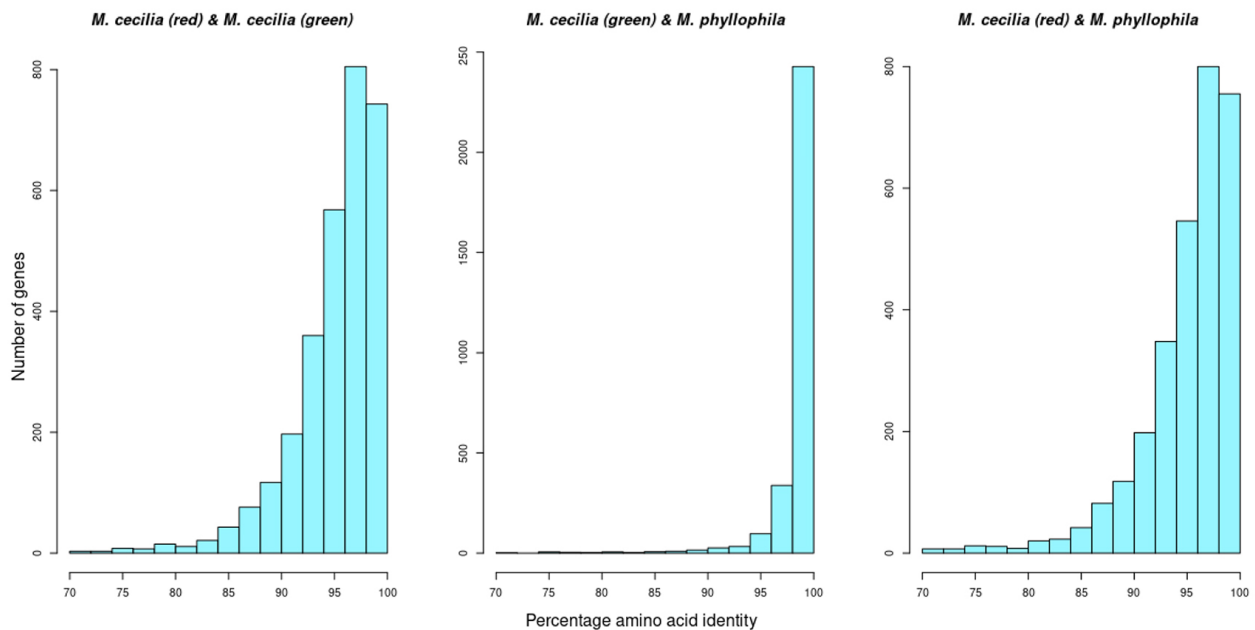


Fig. 5. – Amino acid identity (in percentage) among 2977 orthologous genes.

morphotypes clustered in a single well-supported clade (100%, Fig. 4). The ten best partitions were found by ASAP, but they were not informative (>0.1).

For *16S*, the partial consensus sequence was 586 nt long for both morphotypes. The best-fitting model of substitution was HKY+G. The value of uncorrected p-distance ranged between 0% and 15%. The lowest values were between MCG or MCR vs. other *Mycale* species including *M. (C.) phyllophila* and *M. (C.) cecilia* (Table 1). The number of divergences ranged from 0 to 90 (Table 1). There was no difference between MCR and one of the *M. (C.) cecilia* sequences from Hawaii. Neither the other *M. (C.) cecilia* sequence from Hawaii nor *M. (C.) phyllophila* differed from MCG. There was just one substitution (p-distance = 0.17%) between *M. (C.) cecilia* colour morphotypes. The phylogenetic relationship was not well resolved. Both morphotypes were in a polytomy clade, perhaps because of extremely low divergence values caused by the low substitution rate that this gene shows (see Supplemental Material Fig. S3). The ten best partitions were found by ASAP, but they were not informative (>0.1).

Similarity between red and green morphotype transcriptomes

The sequencing and transcriptome data (NCBI Bioproject PRJNA678333) of morphotypes of *M. (C.) cecilia* are described in detail by Castillo-Páez et al. (2021). In summary, the RNA-seq of six samples yielded ~129 million raw reads with a length of 150 nt. Each morphotype was assembled separately because of the global assembly's low overlap. Transcript totals of 461266 for MCG and 342237 for MCR were obtained. Of these, 153498 (MCG) and 122979 (MCR) were

long ORFs. Only 48023 (MCG) and 37443 (MCR) ORFs had hits with Porifera. The raw RNA-seq reads for the three life cycle stages of *M. (C.) phyllophila* were assembled de novo, and 384743 transcripts were obtained.

Potentially orthologous genes (2977) were recovered by bidirectional best-hit with BLASTP after contrasting the sequences assembled from each morphotype of *M. (C.) cecilia* with the *M. (C.) phyllophila* transcripts and the Porifera ORFs (hereafter referred to as orthologous genes). The percentage of amino acid identity of the 2977 orthologous genes between MCR and MCG was lower than that between MCG and *M. (C.) phyllophila* (Fig. 5). MCR vs. MCG had an average identity of 95.14%: 102 genes were identical, while 245 genes were 99% identical between each data set. This is much lower than the figure for MCG vs. *M. (C.) phyllophila*, which showed an identity of 98.59%: 661 genes showed homology at 100% and 1210 at 99%. The percentage of amino acid identity values of MCR vs. *M. (C.) phyllophila* was quite similar to that of the *M. (C.) cecilia* morphotypes, with an average identity of 95.02%: 106 were identical and 252 were 99%.

Phylogenetic relationships inferred from transcriptomes

The number of transcripts after assembly for *Mycale* species and outgroup ranged from 85915 for *Clathria prolifera* to 299581 for *M. tridens* (see Supplementary Material Table S1). The number of complete proteins ranged from 17184 for *Mycale acerata* to 54915 for *M. laevis*. Only 12 single-copy orthologous genes were present in all species analysed. The phylogenetic reconstruction showed the same patterns as

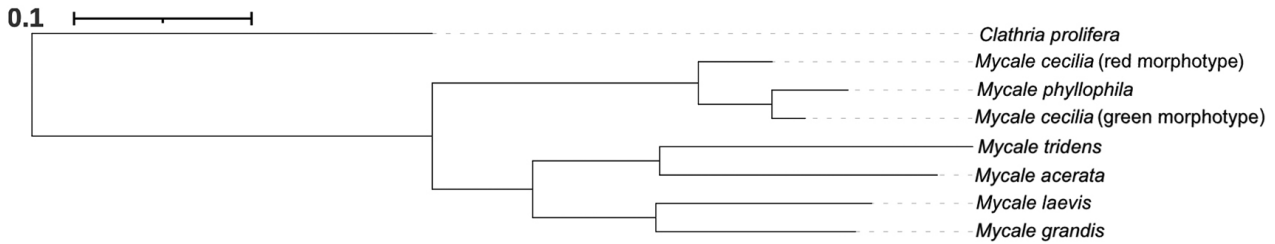


Fig. 6. – Species tree with 12 complete single-copy orthologous genes using STAG inference, where branch lengths represent the average number of substitutions per site across a large range of gene families.

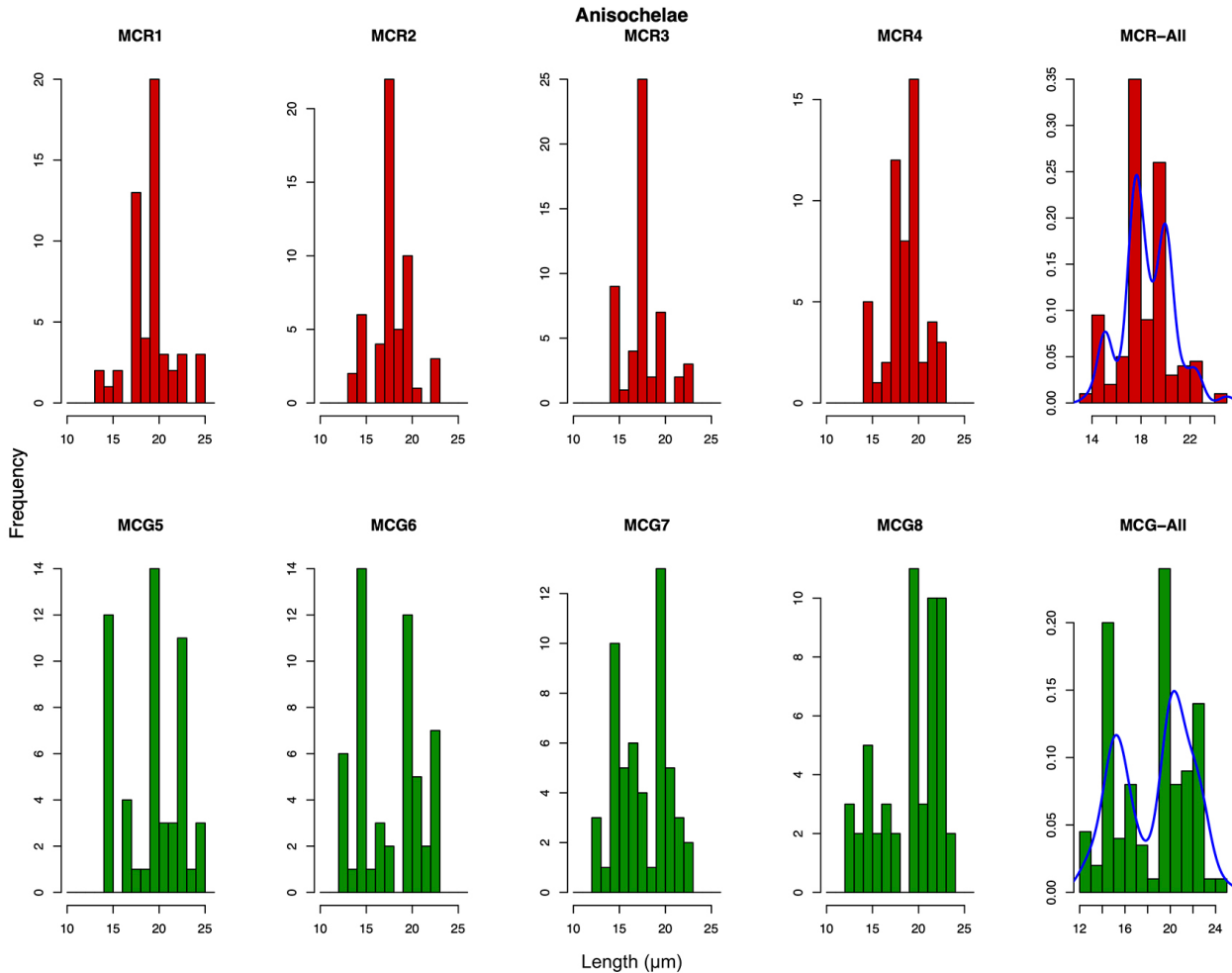


Fig. 7. – The total length-frequency distribution of palmate anisochelae of each individual of *Mycale (C.) cecilia* (MCR, red individuals; MCG, green individuals). Frequency and density (blue line) for grouped individuals of the same colour.

the phylogenetic reconstructions of traditional loci: *M. (C.) phyllophila* appears to be a sister to MCG (Fig. 6). The same pattern was observed when the number of complete genes (75 and 106) was increased by excluding samples that did not have them (see Supplementary Material Fig. S4).

External body shape and colour

Individuals displayed a similar external body shape in life, differing only in coloration. The organisms

were mottled patchwork red to reddish-orange or green to greenish-yellow and covered by a translucent dermal membrane (Fig. 1). They were encrusted about 0.5 cm thick and fine-grained; the consistency was very soft and fragile with a smooth surface.

Spicule morphometry

Regarding the specimens' spicules of both morphotypes (MCR and MCG), the length of mycalostyles ranged from 205 to 300 µm. The averages

varied from 236.7 (individual MCR2) to 261.8 μm (individual MCG5; Table 2). In most individuals, there was a normal distribution in the length-frequency of mycalostyles, but it was most robust when individuals with the same colour were grouped (see Supplementary Material Fig. S5). There were strong significant differences ($F = 6.73$, $p = 3.8e^{-07}$) between the eight individuals analysed and when pooled together with individuals with the same body colour (red vs. green, $F = 24.27$, $p = 1.76e^{-06}$). An a posteriori test revealed that the MCG5 individual was the most different, showing significant differences from three red organisms and from one of the same body colour (green). Furthermore, the shaft width of mycalostyles varied between individuals. It fluctuated from 2.5 μm in both morphotypes to 7.5 μm in the green (MCG5) and 10 μm in the red (MCR2) individuals. The mean ranged from 4.52 (MCG6) to 5.94 μm (MCR2; Table 2). There were significant differences ($F = 5.61$, $p = 6.6e^{-06}$) in the shaft width of mycalostyles. Individual MCR2 was the most different. It varied with

two individuals of the same body colour and with three of the green body colour. Individual MCG6 was different from one individual of each body colour. The other measure we analysed was the width of the head of mycalostyles. It ranged from 2.5 to 7 μm in red individuals and from 3 to 8.75 μm in green individuals. The means ranged from 4.40 (MCG7) to 5.97 μm (MCR2). Significant differences were found between individuals ($F = 6.84$, $p = 2.9e^{-07}$). The MCR2 individual was the most divergent in width of the head of mycalostyles, and it was different for all individuals except for one individual of the different body colour (green).

The length of sigmas ranged from 25 μm in the red and 27.5 μm in the green to 42.5 μm in the organisms of both colours. The average varied from 31.20 (MCR4) to 37.45 μm (MCG7; Table 2). Normal distribution in the frequency was found in most individuals (see Supplementary Material Fig. S6). Significant differences were found between individuals ($F = 8.72$, $p = 2.6e^{-09}$). The individual MCG7 was the most different in sig-

Table 2. – Spicule measures (μm) for each individual of *Mycale* (*C.*) *cecilia* (MC). I and II in palmate anisochelae represent the two categories found only in green individuals.

ID	Body colour	Mycalostyles				Sigma Length	Palmate anisochela length			
		Length	Shaft width	Head width	Length total		Head length			
MCR1	Red	Min.	212.5	2.50	3.75	25.00	13.75		7.50	
		Max.	265.0	7.50	7.50	42.50	25.00		12.50	
		Avg.	238.6	5.03	5.13	33.10	19.28		10.20	
MCR2	Red	Min.	205.0	2.50	3.75	27.50	13.75		7.50	
		Max.	260.0	10.0	8.75	42.50	22.5		12.50	
		Avg.	236.7	5.94	5.97	33.40	18.00		10.10	
MCR3	Red	Min.	215.0	3.00	3.00	27.50	15.00		7.50	
		Max.	300.0	5.50	6.25	41.25	22.50		12.50	
		Avg.	248.6	4.59	4.85	33.70	17.82		10.16	
MCR4	Red	Min.	210.0	2.50	3.00	25.00	15.00		7.50	
		Max.	265.0	7.00	7.50	37.50	22.50		12.50	
		Avg.	242.0	4.57	4.97	31.20	18.88		10.49	
MCG5	Green	Min.	215.0	2.50	3.00	27.50	I	II	I	II
		Max.	300.0	7.50	7.00	41.25	15.00	20.00	6.25	9.50
		Avg.	261.8	5.67	5.36	35.78	18.75	25.00	8.75	13.75
MCG6	Green	Min.	210.0	2.50	2.50	27.50	15.71	21.46	7.56	11.35
		Max.	275.0	5.50	7.00	37.50	12.50	20.00	5.00	9.00
		Avg.	244.1	4.52	4.62	33.75	17.500	22.50	8.75	12.50
MCG7	Green	Min.	205.0	2.50	3.75	33.75	14.81	20.80	6.82	11.06
		Max.	290.0	5.50	5.00	42.50	12.50	20.00	6.25	9.50
		Avg.	253.4	4.56	4.40	37.45	18.75	22.50	8.75	12.50
MCG8	Green	Min.	205.0	2.50	3.00	30.00	15.59	20.43	7.76	10.64
		Max.	280.0	7.00	7.00	40.00	12.50	20.00	6.25	9.50
		Avg.	255.8	4.86	4.81	36.30	17.50	23.75	8.75	12.50

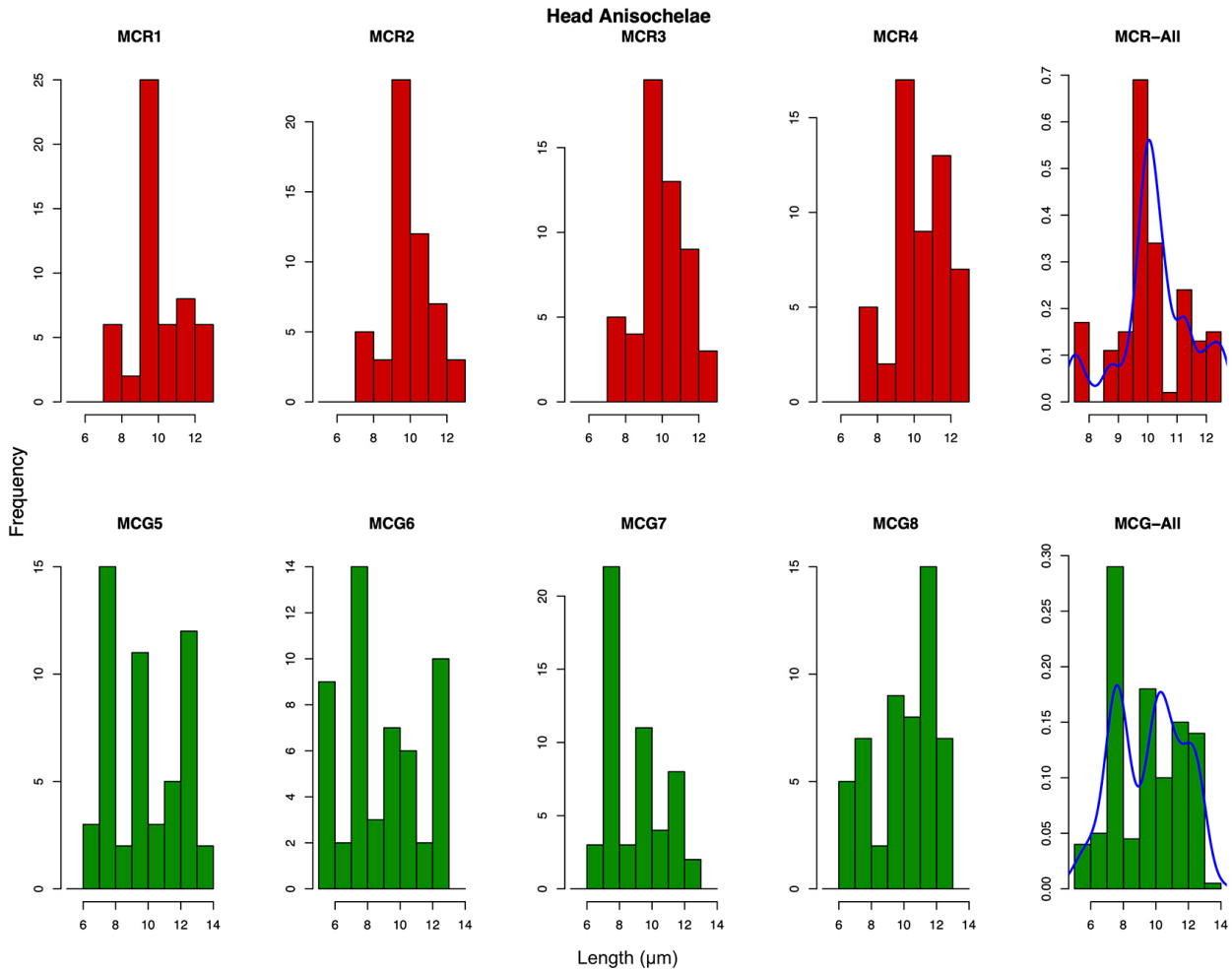


Fig. 8. – The head length-frequency distribution of palmate anisochelae of each individual of *Mycale (C.) cecilia* (MCR, red individuals; MCG, green individuals). Frequency and density (blue line) for grouped individuals of the same colour.

ma length, which varied from all the individuals with red body colour and one with green body colour. We also found highly significant differences ($F = 34.51$, $p = 1.76e^{-08}$) when we collapsed all sigma lengths by colour into a data set and compared them.

The total length range of palmate anisochelae was 13.75 to 25 μm in the red morphotype and 12.5 to 25 μm in the green morphotype (Table 2). The average ranged from 17.72 (MCG7) to 19.51 μm (MCG5). All green individuals had less frequency in length between 16.5 and 19.75 μm (Fig. 7). This possibly corresponds to two categories: Category I, 12.5 to 16.25 μm ; and Category II, 20 to 25 μm . The density curve for grouped green individuals (Fig. 7, MCG-All) was bimodal with a clear gap, but this was not found in grouped red individuals, which did not have a clear gap (MCR-All). Homoscedasticity was solely found when individuals were grouped by colour. Significant differences were found between red individuals ($F = 5.75$, $p = 8.47e^{-04}$), specifically between MCR1-MCR2 and MCR1-MCR3. Green individuals were also significantly different ($F = 5.08$, $2.04e^{-03}$): MCG5-MCG6, MCG5-MCG7 and MCG7-MCG8. The head length of palmate anisochelae

lae ranged from 7.5 to 12.5 μm in the red individuals and from 5 to 13.75 μm in the green individuals (Table 2). The average of the red morphotype was 10 μm , but the green ones ranged between 8.94 and 10.2 μm . The variation pattern in head length matched (or mirrored) the pattern of total length reported above. Only green individuals had less frequency in head length between 8.25 and 9.75 μm (Fig. 8), suggesting that there are two categories: Category I, 6.25 to 8 μm ; and Category II, 10 to 13.75 μm . The density curve for grouped green individuals (Fig. 8, MCG-All) was bimodal. Homoscedasticity was found when individuals were grouped by colour. No significant differences were found between red ($F = 0.99$, $p = 0.39$) individuals and differences ($F = 4.51$, $p = 4.45e^{-03}$) were detected between only MCG8-MCG6 and MCG8-MCG7 green individuals.

No colour morphotype clusters were observed in PCA analyses. This suggests that the measured variables did not help differentiate between morphotypes. The length of the different types of spicules was correlated. However, these values were negatively correlated with the head or shaft width of mycalostyles, suggesting that it is sufficient to measure only the head or shaft

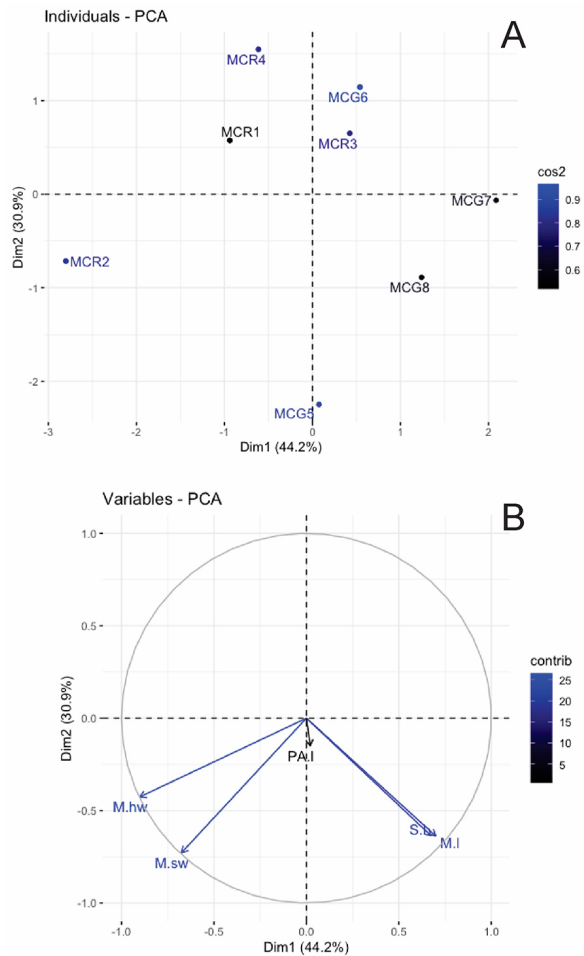


Fig. 9. – Principal component analysis (PCA) based on individuals (A) or variables (B). Colours indicate (A) the individual representability or (B) the contribution of each variable to the principal component. MCR, red individuals; MCG, green individuals; M.l, mycalostyle length; M.s.w, mycalostyle shaft width; M.h.w, mycalostyle head width; S.l, sigma length; P.A.l, palmate anisochela length

width and the length of mycalostyles (Fig. 9). The size of the palmate anisochelae was the variable that contributed least to the morphometric ordination because it did not have a normal distribution, as mentioned above. In conclusion, no clusters by colour morphotype were found, and the variable that contributed the least in the PCA analysis (i.e. anisochelae length) is one of those that shows an evident difference in the histogram analysis.

DISCUSSION

From the original description of *M. (C.) cecilia* by de Laubenfels (1936) to subsequent reports by the same author (de Laubenfels 1950), there are likely many cryptic species in what is currently known as *M. (C.) cecilia*. The main difficulty in the species delimitation is that members of this species inhabit the same envi-

ronment, and the individuals are very similar in morphology, with the same types and sizes of spicules and skeletal organization. Integrative taxonomy that incorporates information from different sources (molecular, morphological, and others) has allowed the discovery of cryptic species not only in poriferans. Cryptic species discovery has also been reported in other marine groups, such as mollusks and arthropods. It is important to recognize cryptic species in an evolutionary and ecological context because they represent a challenge for management and biodiversity estimates for both their communities and the nominal species (Chenauil et al. 2019). Here we integrate molecular and morphological analysis to provide evidence that strongly supports cryptic speciation in at least two sympatric morphotypes of *M. (C.) cecilia* in Mazatlán, Mexico. First, two size categories of palmate anisochelae were found in MCG and only one in MCR organisms. Second, we found that individuals with the same body colour had the same *ITS1* sequence, and the sequences were highly divergent between morphotypes. Third, there is a concordance in all nuclear and mitochondrial phylogenetic reconstructions, as MCG clustered with *M. (C.) phyllophila* instead of MCR (except for the D3-D5 domain of 28S rRNA), and the genetic distances between MCG and *M. (C.) phyllophila* were the lowest. Fourth, each morphotype was assigned to a different subset in species delimitation analysis for *ITS*. Fifth, at the transcriptomic level, the MCG was more related to another *M. (C.) phyllophila* species than the MCR. Therefore, our study suggests that *M. (C.) cecilia* individuals can be misidentified if only their morphological characteristics are considered. Although we found that the body colour and the differences in the palmate anisochela categories could be diagnostic characteristics to separate the green and red morphotypes, further studies should be carried out to discriminate the other colour morphotypes not evaluated here (for example, blue and yellow body colours). In species with low phenotypic variability, it is essential to use more than one tool (morphometric and molecular markers) for a robust analysis.

Congruence in nuclear and mitochondrial traditional loci

Molecular markers have been established as powerful tools for revealing the biodiversity of “hidden” marine sponges, such as cryptic or complex species that cannot be resolved with only morphological characters (Uriz and Turon 2012, Shaffer et al. 2019). In some sponge studies, nuclear gene fragments have been more informative than mitochondrial ones (Bucklin et al. 2011, Uriz and Turon 2012). Partial *ITS1* nuclear locus showed low genetic variation levels within *M. (C.) cecilia* morphotypes and high variation between them. Surprisingly, the sequence of *M. (C.) phyllophila* organisms collected from China was more closely related to the MCG. The sequences of *M. (C.) phyllophila* were quite similar to the MCG sequences, with genetic distances and the number of substitutions being

the lowest in the pairwise comparisons and clustered in a highly supported clade. However, in the species delimitation analysis, *M. (C.) phyllophila* and MCG appeared to belong to different species because they were included in different subsets. The same occurred with the two morphotypes of *M. (C.) cecilia* where the MCR sequences were grouped into a single subset and the MCG sequences into another subset. These results indicate that each morphotype belongs to a different species. Park et al. (2007) suggest that the *ITS* region (*ITS1* and *ITS2*) could be more appropriate for molecular barcoding in sponges than mitochondrial genes. They indicated that the *ITS1* locus exhibited the highest levels of intra- and interspecific variation in uncorrected p-distances compared with *ITS2* and 5.8S. Intraspecific (1.52%) and interspecific (17.28%) maximum values of genetic divergence for Halichondriidae were an order of magnitude higher (Park et al. 2007). The same pattern was observed for *Suberites diversicolor*. The average p-distance within the lineages (lineage A 0.25% or lineage B 0.44%) was lower than that between lineages (7.26%) (Becking et al. 2013), and similar values were found in the morphotypes of *M. (C.) cecilia* (0.3% intra- and 8.78% inter-lineage). *ITS1* could be useful for taxonomic identification and genetic divergence for the other body colour morphotypes registered for *M. (C.) cecilia* and could be extended to other species of *Mycale*.

We obtained two domains of the 28S rRNA of the transcriptome. The D1-D2 domain was useful and matched with the phylogenetic reconstructions of another nuclear marker (*ITS1*). The genetic distance between morphotypes was low but not the lowest. MCG and *M. (C.) phyllophila* clustered in a strongly supported clade and were included in the same subset, suggesting that *M. (C.) phyllophila* could be a sister or the same species to the green morphotype. This extremely low divergence was recorded in another sponge group where only one substitution between *Pachymatisma johnstonia* and *Pachymatisma normani* was found for this domain (Cárdenas et al. 2010). Borchiellini et al. (2000) suggest that the D1-D2 domain appears more informative and provides better resolution for internal topologies in sufficiently closely related species. The genus *Hemimycal* was the only phylogenetic reconstruction with monophyly and low bootstrap value (Uriz et al. 2017). Cárdenas et al. (2010) used D1-D2 and D3-D5 of the 28S rRNA and *COX1* to evaluate the phylogeny of Geodiidae. They observed patterns similar to those found in *M. (C.) cecilia*. First, there was extremely low divergence in the D1-D2 domain and *COX1*, and the D3-D5 phylogeny was inconsistent with the D1-D2 domain and *COX1*. The authors suggest that the D3-D5 domain could evolve quite differently from *COX1* and the D1-D2 domain. Furthermore, they suggest that the latter could be an excellent nuclear marker for barcode rather than *COX1*. This is exactly what happened among the morphotypes of *M. (C.) Cecilia*. We found D1-D2 had more substitutions than *COX1*, and there was phylogeny of the D3-D5 incongruence.

The *COX1* and I3-M11 partitions are commonly used for species delimitation and population structure research. *COX1* is also a marker of slow evolution in sponges and sometimes fails to resolve phylogenetic relationships and speciation (Belinky et al. 2012; see Uriz and Turon 2012). Though both morphotypes of *M. (C.) cecilia* showed only seven substitutions in 1261 nt, and five of them were in the first 717 nt, the phylogenetic relationship (Fig. 4) between morphotypes was well resolved. In 99% of the phylogenetic reconstructions, MCG was clustered with *M. (C.) phyllophila*, rather than MCR. The genetic divergence between the morphotypes of *M. (C.) cecilia* was low (0.5) when compared with other *Mycal* species, except for the green morphotype and *M. (C.) phyllophila*, which was zero. A lower value than this was obtained between lineage A and B for *S. diversicolor*, where the divergence was 0.38 (Becking et al. 2013).

The nuclear 18S rRNA gene and the mitochondrial 16S rRNA were non-informative in our phylogenetic reconstructions and speciation delimitation. However, the trees have similar patterns to the other phylogenetic reconstructions. All subsets of different partitions overlapped well-defined species, indicating the low resolution for species delimitation. Borchiellini et al. (2000) suggest that 18S rRNA loci are not informative for resolving relationships between genera.

Our molecular findings are opposite to those found in the congener *M. (Mycal) laevis*, where four morphotypes (orange or white, semi-cryptic or massive) showed no genetic differences, suggesting that they all constitute a single species (Loh et al. 2012). This finding is relevant because it suggests that body colour is unrelated to genetic similarity. There could be more *Mycal* species with very low levels of divergence and they are probably unpredictable when evaluated by few genes. However, the molecular markers used may not have been sufficiently informative. It would be interesting to assay this species again using the *ITS1*, 28S rRNA D1-D2 and *COX1*.

Reports of cryptic sympatric speciation in sponges have increased in recent years in different groups of marine sponges. Cryptic species are widespread across Porifera (Knapp et al. 2015). Both mitochondrial and nuclear markers revealed at least three different species for the only known *Scopalina lophyropoda*, as in the case of our *M. (C.) cecilia*. *Scopalina blanensis* can even be found in contact with the true *S. lophyropoda*. These species of *Scopalina* also have little morphological differentiation including coloration: bright brownish orange in *S. lophyropoda* and salmon-orange in *S. blanensis* (Blanquer and Uriz 2008). Individuals of *Haliclona (Soestella) caerulea* species were morphologically indistinguishable, but in mitochondrial analysis, haplotypes can be up to 13.9% divergent, and even in the concatenated mitochondrial and nuclear tree they revealed two major clades (Knapp et al. 2015).

Morphotypes similarity at the transcriptome level

Our study is probably the first assessment at the transcriptomic level for species delimitation in marine sponges. Where we found the same results in individ-

ual genes, we found much more divergence than expected between the two *M. (C.) cecilia* morphotypes. The global assembly (all reads of *M. (C.) cecilia* morphotypes) had a low overlap between body colour morphotypes, suggesting a high degree of divergence between them. Further, the average amino acid identity of the orthologous genes between MCR and MCG (95.14%) was much lower than that between MCG and *M. (C.) phyllophila* (98.59%); thus, many of these orthologous genes were more identical between MCG and *M. (C.) phyllophila*. The same was true in the phylogenetic reconstruction of the complete genes of the transcriptomes with different *Mycale* species. The phylogenetic reconstructions of 12, 75 and 106 complete single-copy orthologous genes show the same pattern among them and with the trees of traditional genes. Namely, both *M. (C.) cecilia* morphotypes and *M. (C.) phyllophila* clustered but the green morphotype appears to be a sister to the *M. (C.) phyllophila* in place of the red morphotype.

The number of orthologous genes found among the three species (*M. (C.) cecilia* morphotypes and *M. (C.) phyllophila*) was quite similar to that found in recent research. In the phylogenomic inference of the Spongillidae, 2710 orthogroups were detected among 11 sponge species. These concatenated orthologous genes were enough to reveal conclusively the inter-relationships of freshwater sponges (Kenny and Itskovich 2020).

The results obtained from the transcriptome comparison of MCG vs. *M. (C.) phyllophila* were unexpected. Firstly, the coloration of *M. (C.) phyllophila* is red; so, we would expect it to be more similar to MCR, but the opposite was found. Second, we did not expect a high level of similarity in the identity of the amino acid of orthologous genes between MCG and *M. (C.) phyllophila* (98%). We expected the similarity to have a similar value to other species comparisons (95%). This great similarity is interesting because *M. (C.) phyllophila* was sampled in China and MCG in Mexico. So far, it is unclear why two species that inhabit areas almost 8000 miles apart are much more similar than those that coexist.

Consistent morphological differences

Following the original description of *M. (C.) cecilia*, both Mazatlán morphotypes (red and green) had mycalostyles in a single size category, without apparent differences between them. These mycalostyles were slightly smaller and narrower than those of the Panama individuals but similar to those from Hawaii (see the Introduction and Table 2). Both morphotypes had sigmas in a single size category without length differences. The sigmas were also identical in size to specimens from Panama and Hawaii. Two green individuals, one for mycalostyle length and one for sigma length, were different even with individuals of the same body colour, suggesting that other spicular measurements overlapped between morphotypes. Further, we found differences between morphotypes when the analysis was done in body colour pools, i.e.

all the measures without considering the individuals, only the body colour. We did not find morphotype clusters in PCA analysis, suggesting that spicule morphometry was unsuitable for delimiting morphs, even when some of them were correlated by length. The main spicule difference between morphotypes, and perhaps the most significant diagnostic key, along with coloration, was the presence/absence of two discrete categories in the total and head length of palmate anisochelae. According to de Laubenfels (1936), the type material of *M. (C.) cecilia* was green in life and showed two size categories of palmate anisochelae, which seems similar to our green specimens. The red ones only showed a single anisochela category. de Laubenfels (1950) reported Hawaii individuals with different colourations (pink and lavender or yellow and orange), but without differences in anisochela lengths. Some authors have argued that spicule size categories can be useful as a diagnostic character (Hajdu and Rützler 1998). We suggest then that the colour differences, along with the presence/absence of anisochela size categories, could provide sufficient morphological arguments to separate the two morphotypes into different species, but perhaps they are not the only ones.

We must consider whether other body colour morphotypes (i.e. orange, yellow and blue) recorded along the *M. (C.) cecilia* distribution (Tropical Eastern Pacific and Hawaii) could be different species, especially red and orange morphotypes because they have widespread distribution (Carballo and Cruz-Barraza 2010). Commonly, coloration has been considered to be without taxonomic value in sponge systematics because the colour could vary as a function of the environmental conditions or when the animals are moved from one place to another (Park et al. 2007, Blanquer and Uriz 2008). Nevertheless, in some species identification, the body colour could be used as an additional character, especially when colour differences are slight but constant (Blanquer and Uriz 2008, Esteves et al. 2018).

According to our results, it is possible to attribute the green individuals to the *M. (C.) cecilia* species. These specimens shared the colouration and the presence of two anisochela categories described by de Laubenfels. In contrast, we found that the red individuals could correspond to another species of *Mycale*, perhaps a new species. To confirm whether the MCR is a new species, the other colour morphotypes described in the *M. (C.) cecilia* distribution and other species belonging to the genus *Mycale* need to be examined. It is possible that these (red and green) and other morphotypes described for *M. (C.) cecilia* in the same geographic location could be involved in a species complex because they are closely related and morphologically very similar, but the boundaries between them are unclear. We shall continue working to unravel the phenotypic plasticity bases of *M. (C.) cecilia* cryptic species at different levels, including genetic markers and gene expression profiles, to improve our knowledge of this species complex.

SUPPLEMENTARY MATERIAL

The following supplementary material is available through the online version of this article and at the following link:

Fig. S1. – Maximum likelihood phylogenetic reconstruction of the partial D3-D5 domain of the 28S gene among morphotypes of *Mycale (C.) cecilia* (MCR, red individuals; MCG, green individuals) and other species of *Mycale*. Values in the nodes indicate bootstrap support (300 replicates). GenBank accession numbers are in parentheses. No bootstrap values because they are less than 75%.

Fig. S2. – Maximum likelihood phylogenetic reconstruction of the nuclear 18S gene among morphotypes of *Mycale (C.) cecilia* (MCR, red individuals; MCG, green individuals) and other species of *Mycale*. Values in the nodes indicate bootstrap support (>75%, 300 replicates). GenBank accession numbers are in parentheses.

Fig. S3. – Maximum likelihood phylogenetic reconstruction of 16S gene among morphotypes of *Mycale (C.) cecilia* (MCR, red individuals; MCG, green individuals) and other species of *Mycale*. Values in the nodes indicate bootstrap support (>75%, 300 replicates). GenBank accession numbers are in parentheses.

Fig. S4. – Species tree of complete single-copy orthologs using STAG inference, where branch lengths represent the average number of substitutions per site across a large range of gene families. A, 75 complete genes; B, 106 complete genes.

Fig. S5. – Length-frequency distribution of mycalostyles of each individual of *Mycale (C.) cecilia* (MC).

Fig. S6. – Length-frequency distribution of sigmas of each individual of *Mycale (C.) cecilia* (MC)

Table S1. – Source data for transcriptome phylogenetic analyses.

Table S2. – Commands used in the workflow for transcriptome analysis.

ACKNOWLEDGEMENTS

We thank Adrian Flores for providing two *ITS1* sequences, Benjamin Yañez for the support in collecting samples, Carlos Suarez for computer support, and Karen Englander and Josephine Carubia for reviewing the English text. The first author benefited from a fellowship from UNAM-DGAPA to support her postdoc at UNAM-ICMyL.

DECLARATION OF COMPETING INTEREST

The authors of this article declare that they have no financial, professional or personal conflicts of interest that could have inappropriately influenced this work.

FUNDING SOURCES

This work was funded by PAPIIT (Programa de Apoyo a Proyectos de Investigación e Innovación Tecnológica, DGAPA): PAPIIT-UNAM IN210018 (awarded to José Antonio Cruz-Barraza). Ana Castillo-Páez benefited from a fellowship from UNAM-DGAPA to support her postdoc at UNAM-ICMyL.

AUTHORSHIP CONTRIBUTION STATEMENT

Ana Castillo-Páez: Conceptualization, Data curation, Formal analysis, Investigation, Methodology, Software, Visualization, Writing – original draft, review and editing. Raúl Llera-Herrera: Conceptualization, Data curation, Formal analysis, Investigation, Methodology Software, Visualization, Writing – review & editing. José Antonio Cruz-Barraza: Conceptualization, Data curation, Funding acquisition, Investigation, Methodology, Project administration, Resources, Supervision, Writing – review & editing.

REFERENCES

Aldard R., Lester R.J. 1995. Development of a diagnostic test for *Mikrocytos roughleyi*, the aetiological agent of Australian winter mortality of the commercial rock oyster, *Saccostrea commercialis* (Iredale and Roughley). *J. Fish Dis.* 18: 609-614.
<https://doi.org/10.1111/j.1365-2761.1995.tb00365.x>
Becking L.E., Erpenbeck D., Peijnenburg K.T.C.A., de Voogd N.J. 2013. Phylogeography of the Sponge *Suberites diver-*

sicolor in Indonesia: Insights into the Evolution of Marine Lake Populations. *PLoS ONE* 8: e75996

<https://doi.org/10.1371/journal.pone.0075996>

Belinky F., Szitenberg A., Goldfarb I., et al. 2012. ALG11 - A new variable DNA marker for sponge phylogeny: Comparison of phylogenetic performances with the 18S rDNA and the COI gene. *Mol. Phylogenet. Evol.* 63: 702-713.
<https://doi.org/10.1016/j.ympev.2012.02.008>

Bickford D., Lohman D.J., Sodhi N.S., Ng P.K.L., Meier R., Winker K., Ingram K.K., Das I. 2006. Cryptic species as a window on diversity and conservation. *Trends Ecol. Evol.* 22: 148-155.
<https://doi.org/10.1016/j.tree.2006.11.004>

Blanquer A., Uriz M-J. 2007. Cryptic speciation in marine sponges evidenced by mitochondrial and nuclear genes: A phylogenetic approach. *Mol. Phylogenet. Evol.* 45: 392-397.
<https://doi.org/10.1016/j.ympev.2007.03.004>

Blanquer A., Uriz M-J. 2008. “A posteriori” searching for phenotypic characters to describe new cryptic species of sponges revealed by molecular markers (Dictyonellidae: Scopalina). *Invertebr. Syst.* 22: 489-502.
<https://doi.org/10.1071/IS07004>

Borchiellini C., Chombar C., Lafay B. NB-E. 2000. Molecular systematics of sponges (Porifera). *Hydrobiologia.* 420: 15-27.
https://doi.org/10.1007/978-94-017-2184-4_2

Bucklin A., Steinke D., Blanco-Bercial L. 2011. DNA Barcoding of Marine Metazoa. *Ann. Rev. Mar. Sci.* 3: 471-508.
<https://doi.org/10.1146/annurev-marine-120308-080950>

Carballo J.L., Cruz-Barraza J.A. 2008. First record of *Axinysa Lendenfeld, 1897* (Demospongiae, Halichondrida) from the East Pacific Ocean, with the description of *Axinysa isabela* sp. nov. *Zootaxa.* 1784: 58-68.
<https://doi.org/10.11646/zootaxa.1784.1.4>

Carballo J.L., Cruz-Barraza J.A. 2010. A revision of the genus *Mycale* (Poecilosclerida: Mycalidae) from the Mexican Pacific Ocean. *Contrib. Zool.* 79: 165-191.
<https://doi.org/10.1163/18759866-07904003>

Cárdenas P., Pérez T., Boury-Esnault N. 2012. Sponge Systematics Facing New Challenges. *Adv. Mar. Biol.* 61: 79-209.
<https://doi.org/10.1016/B978-0-12-387787-1.00010-6>

Cárdenas P., Rapp H.T., Schander C., Tendal O.S. 2010. Molecular taxonomy and phylogeny of the Geodiidae (Porifera, Demospongiae, Astrophorida) - Combining phylogenetic and Linnaean classification. *Zool. Scr.* 39: 89-106.
<https://doi.org/10.1111/j.1463-6409.2009.00402.x>

Castillo-Páez A.Y., Llera-Herrera R., Cruz-Barraza J.A. 2021. De novo transcriptome assembly for two colour types of the marine sponge *Mycale (Carmia) cecilia*. *Mol. Biol. Rep.* 48: 1-4.
<https://doi.org/10.1007/s11033-021-06274-4>

Chenaui A., Cahill A.E., Délémontey N., et al. 2019. Problems and questions posed by cryptic species. A framework to guide future studies. In: Casetta J., da Silva., Vecchi D. (eds), *From Assessing to Conserving Biodiversity: Conceptual and Practical Challenges*, pp. 77-106.
https://doi.org/10.1007/978-3-030-10991-2_4

Desqueyroux-Faúndez R., van Soest R.W.M. 1997. Shallow waters Demosponges of the Galápagos Islands. *Rev. Suisse Zool.* 104: 379-467.
<https://doi.org/10.5962/bhl.part.80003>

Emms D.M., Kelly S. 2017. STRIDE: Species Tree Root Inference from Gene Duplication Events. *Mol. Biol. Evol.* 34: 3267-3278.
<https://doi.org/10.1093/molbev/msx259>

Emms D.M., Kelly S. 2018. STAG: Species Tree Inference from All Genes. *BioRxiv.* 267914.
<https://doi.org/10.1101/267914>

Emms D.M., Kelly S. 2019. OrthoFinder: Phylogenetic orthology inference for comparative genomics. *Genome Biol.* 20: 1-14.
<https://doi.org/10.1186/s13059-019-1832-y>

Escobar D., Zea S., Sánchez J.A. 2012. Phylogenetic relationships among the Caribbean members of the *Cliona viridis* complex (Porifera, Demospongiae, Hadromerida) using nuclear and mitochondrial DNA sequences. *Mol. Phylogenet. Evol.* 64: 271-284.
<https://doi.org/10.1016/j.ympev.2012.03.021>

Esteves E.L., de Paula T.S., Lerner C., et al. 2018. Morphological and molecular systematics of the “*Monanchora ar-*

- buscula* complex” (Poecilosclerida: Crambeidae), with the description of five new species and a biogeographic discussion of the genus in the Tropical Western Atlantic. *Invertebr. Syst.* 32: 457-503.
<https://doi.org/10.1071/IS16088>
- Fusco G., Minelli A. 2010. Phenotypic plasticity in development and evolution: facts and concepts. *Philos. Trans. R. Soc. Lond., B, Biol. Sci.* 365: 547-556.
<https://doi.org/10.1098/rstb.2009.0267>
- Green G., Gómez P. 1985. Estudio taxonómico de las esponjas de la Bahía de Mazatlán Sinaloa, México. *An. Cent. Cienc. Mar. Limnol.* 273-300.
- Haas B.J., Papanicolaou A., Yassour M., et al. 2013. *De novo* transcript sequence reconstruction from RNA-seq using the Trinity platform for reference generation and analysis. *Nat. Protoc.* 8: 1494-1512.
<https://doi.org/10.1038/nprot.2013.084>
- Hajdu E., Riitzler K. 1998. Sponges, genus *Mycale* (Poecilosclerida: Demospongiae: Porifera), from a Caribbean mangrove and comments on subgeneric classification. *Proc. Biol. Soc. Wash.* 111: 737-773.
- Huang D., Meier R., Todd P.A., Chou L.M. 2008. Slow mitochondrial COI sequence evolution at the base of the metazoan tree and its implications for DNA barcoding. *J. Mol. Evol.* 66: 167-174.
<https://doi.org/10.1007/s00239-008-9069-5>
- Kenny N.J., Itskovich V.B. 2020. Phylogenomic inference of the interrelationships of Lake Baikal sponges. *Syst. Biodivers.* 0: 1-9.
- Knapp I.S., Forsman Z.H., Williams G.J., et al. 2015. Cryptic species obscure introduction pathway of the blue Caribbean sponge (*Haliclona* (*Soestella*) *caerulea*), (order: Haplosclerida) to Palmyra Atoll, Central Pacific. *PeerJ.* 2015.
<https://doi.org/10.7717/peerj.1170>
- Knowlton N. 1993. Sibling species in the sea. *Annu. Rev. Ecol. Syst.* 24: 189-216.
<https://doi.org/10.1146/annurev.es.24.110193.001201>
- Kumar S., Stecher G., Li M., et al. 2018. MEGA X: Molecular evolutionary genetics analysis across computing platforms. *Mol. Biol. Evol.* 35: 1547-1549.
<https://doi.org/10.1093/molbev/msy096>
- de Laubenfels M.W. 1936. A comparison of the shallow-water sponges near The Pacific and of The Panama Canal with those at The Caribbean end. *Proc. U. S. Natl. Mus.* 83: 441-466.
<https://doi.org/10.5479/si.00963801.83-2993.441>
- de Laubenfels M.W. 1950. The sponges of Kaneohe Bay, Oahu. *Pac. Sci.* 4: 3-36.
- Loh T.L., López-Legentil S., Song B., Pawlik J.R. 2012. Phenotypic variability in the Caribbean Orange Icing sponge *Mycale laevis* (Demospongiae: Poecilosclerida). *Hydrobiologia.* 687: 205-217.
<https://doi.org/10.1007/s10750-011-0806-1>
- López-Legentil S., Erwin P.M., Henkel T.P., et al. 2010. Phenotypic plasticity in the Caribbean sponge *Callispongia vaginalis* (Porifera: Haplosclerida). *Sci. Mar.* 74: 445-453.
<https://doi.org/10.3989/scimar.2010.74n3445>
- Ortega M.J., Zubía E., Sánchez M.C., et al. 2004. Structure and cytotoxicity of new metabolites from the sponge *Mycale cecilia*. *Tetrahedron.* 60: 251-2524.
<https://doi.org/10.1016/j.tet.2004.01.056>
- Park M-H.H., Sim C-J.J., Baek J., Min G-S.S. 2007. Identification of genes suitable for DNA barcoding of morphologically indistinguishable Korean Halichondriidae sponges. *Mol. Cells.* 23: 220-227.
- Petit R.J., Excoffier L. 2009. Gene flow and species delimitation. *Trends Ecol. Evol.* 24: 386-393.
<https://doi.org/10.1016/j.tree.2009.02.011>
- Pfenninger M., Schwenk K. 2007. Cryptic animal species are homogeneously distributed among taxa and biogeographical regions. *BMC. Evol. Biol.* 7: 1-6.
<https://doi.org/10.1186/1471-2148-7-121>
- Puillandre N., Brouillet S., Achaz G. 2021. ASAP: assemble species by automatic partitioning. *Mol. Ecol. Resour.* 21: 609-620.
<https://doi.org/10.1111/1755-0998.13281>
- De Queiroz K. 2007. Species concepts and species delimitation. *Syst. Biol.* 56: 879-886.
<https://doi.org/10.1080/10635150701701083>
- Shaffer M.R., Davy SK., Bell J.J. 2019. Hidden diversity in the genus *Tethya*: comparing molecular and morphological techniques for species identification. *Heredity.* 122: 354-369.
<https://doi.org/10.1038/s41437-018-0134-6>
- Van Soest R.W.M.M., Hajdu E. 2002. Family Mycalidae Lundbeck, 1905. In: Hooper J.N.A., Van Soest R.W.M. (eds), *Systema Porifera: A Guide to the Classification of Sponges*. Kluwer Academic/Plenum Publishers, New York, pp. 669-690.
https://doi.org/10.1007/978-1-4615-0747-5_73
- Uriz M.J., Turon X. 2012. Sponge ecology in the molecular era. *Adv. Mar. Biol.* 61: 345-410.
<https://doi.org/10.1016/B978-0-12-387787-1.00006-4>
- Uriz M.J., Garate L., Agell G. 2017. Molecular phylogenies confirm the presence of two cryptic *Hemimycale* species in the mediterranean and reveal the polyphyly of the genera *Crella* and *Hemimycale* (Demospongiae: Poecilosclerida). *PeerJ* 5:e2958.
<https://doi.org/10.7717/peerj.2958>